ELSEVIER

www.elsevier.nl/locate/carres

Carbohydrate Research 328 (2000) 165–176

CARBOHYDRATE RESEARCH

The phase transformations in starch during gelatinisation: a liquid crystalline approach

Thomas A. Waigh [a,1], Michael J. Gidley [b], Bernard U. Komanshek [c], Athene M. Donald [a,*]

[a] *Polymers and Colloids, Cavendish Laboratory, Cambridge CB3 0HE, UK*
[b] *Unilever Research, Sharnbrook, Bedford MK44 1LQ, UK*
[c] *Daresbury Laboratory, Warrington, Cheshire WA4 4AD, UK*

Received 25 June 1999; received in revised form 3 March 2000

Abstract

The analogy between starch and a chiral side-chain polymeric liquid crystal is examined in relation to the processes involved during gelatinisation. There are three important parameters for characterisation of the molecular phase behaviour of the amylopectin: the lamellar order parameter (ψ), the orientational order parameter of the amylopectin double helices (ϕ), and the helicity of the sample (h, the helix/coil ratio, a measure of the helix–coil transition of the double helices). The coupling between the double helices and the backbone through the flexible spacers is affected dramatically by the water content and it is this factor which dictates the particular phase adopted by the amylopectin inside the starch granule as a function of temperature. SAXS, WAXS and ^{13}C CP/MAS NMR are used to examine these phenomena in excess water. Furthermore, previous experimental evidence pertaining to the limiting water case is reviewed with respect to this new theoretical framework.

Keywords: Starch; Liquid crystalline; X-ray; NMR; Helix–coil transition

1. Introduction

The gelatinisation of the native starch granule is required in almost all culinary and industrial uses of starch [1]. Gelatinisation leads to a change in organisation of the granules as a function of temperature and water content. The phase transitions involved are only slowly being unravelled, in a large part hampered by the lack of understanding of the native granule structure. Previously we have presented evidence that starch has many physical properties in common with a chiral side-chain liquid–crystalline polymer, and it is this analogy relating to the process of gelatinisation that we develop in the present paper [2–4].

The structure of wild type starch is now thought to be hierarchically organised on four length scales [5]: molecular scale ($\sim$ Å), lamellar structure ($\sim$ 90 Å); growth rings ($\sim$ 0.1 μm) and the whole granule morphology ($\sim$ μm). The crystalline regions consist of double helices of amylopectin, which are arranged in either A or B type unit cells [6,7]. The lamellae are alternating regions of amorphous and crystalline material whose total periodicity is 90 Å in all species yet examined [8]. The growth rings are alternating ring structures consisting of amorphous and crys-

* Corresponding author. Fax: +44-1223-337000.
E-mail address: amd3@phy.cam.ac.uk (A.M. Donald).
[1] Present address: Department of Physics, Polymers and Complex Fluids, University of Leeds, Leeds LS2 9JT, UK.

0008-6215/00/$ - see front matter
PII: S0008-6215(00)00098-7

talline regions [5]. The whole granule morphology depends sensitively on the species and takes the form of polyhedra, ellipsoids and spheres [9]. The chiral side-chain liquid–crystalline model for starch considers that an amylopectin molecule consists of three sections: the chiral double helices, the amorphous spacers and the amorphous backbone. It is postulated that the crystalline smectic lamellar periodicity (the alternating regions of crystalline and amorphous material observed in SAXS and electron microscopy experiments [10]) is due to the antagonistic effect of the entropy of the backbone and the ordering of the helices [3]. To maximise the entropy of the water plasticised polymer backbone, the glucose double helices are pushed in to their lamellar structure.

All the four length scales are thought to contribute to the gelatinisation phenomena. The detailed mechanisms involved prove to be surprisingly subtle and hard to elucidate even after exhaustive DSC [11], SAXS [12], SANS [13], DMA [14], optical microscopy [15], and NMR [16] investigations have been conducted. These difficulties are encapsulated in the large number of independent variables involved: species, growth conditions, extraction procedures, water content, heating rate, thermal history, and also due to the malevolent influence of thermodynamic irreversibility [17]. The study of Jenkins and co-workers [18] provides a fair example of the current state of understanding of gelatinisation. In excess water the first step is for the amorphous growth rings to suck in water and rapidly expand in size. Consequently, since the system is widely cross-linked through the amorphous backbone, the coupled semi-crystalline lamellae are then disrupted reducing the granule's crystallinity and causing it to lose its birefringence, which is a measure of the ordering on a length scale of the wavelength of light ~ 0.5 μm. In limiting water the swelling capability of the granule is reduced. Initially some crystallinity is lost by the swelling process described for gelatinisation in excess water. There is however insufficient water to permit full swelling and crystallite disruption. As the temperature is raised, the crystallites remaining undergo a conventional melting transition, leading to an additional DSC endotherm.

In this paper the gelatinisation behaviour of waxy maize, maize and potato starch were monitored in excess water with SAXS/WAXS. The extension to previous studies is that identical samples to those used in a solid state ^{13}C CP/MAS NMR experiment [16] were examined. Therefore conclusions could be drawn using a combination of these probes on the molecular processes involved in gelatinisation. Furthermore, starch/water systems were slowly heated to temperatures around the gelatinisation point, and then cooled back to room temperature. Characterisation of these samples enabled the reversibility of the transformations during gelatinisation in excess water to be deduced.

In addition to this experimental study, a model is presented which relates the phenomena of gelatinisation to the liquid crystalline properties of starch [2–4] as dictated by the order parameters and the degree of mobility of the different sections of the amylopectin. Although the study is preliminary in nature it is important to examine the effect of helix–coil transitions [19,20], and how they relate to the existence of liquid crystallinity.

2. Experimental

Identical samples were provided to those examined by Cooke and Gidley using ^{13}C CP/MAS NMR [16]. Waxy maize, maize and potato starch (5% w/w starch–water) were heated slowly to target temperatures in the range 50–71 °C (i.e., temperatures in the range of the single DSC endotherms observed with these starches in excess water [11]), over a period of 20–30 min followed by rapid cooling and lyophilisation. SAXS/WAXS data were collected on beam line 8.2 at the SRS (Daresbury, UK) from these partially cooked samples, so that the extent to which both long and short range order had been destroyed by the heat treatment could be assessed. [This assumes that only small changes associated with long term room temperature (rt) storage had occurred; the maximum temperatures used were below the end of the gelatinisation endotherm, so that some granule integrity was left. The samples had been stored at rt for a

six month period and the molecular relaxation processes involved in retrogradation would be expected to be complete.

Native starches from identical sources were obtained for dynamic gelatinisation X-ray experiments. The in situ DSC ramp rate in these experiments for dynamic gelatinisation runs was 2 °C/min from 25 to 120 °C. Samples were held in customised DSC cells with mica windows [12]. A particular advantage of the high flux (4×10^{10} ph s^{-1}) and the low noise multi-wire detectors available at Daresbury is the possibility of following transitions in starch dynamically in situ in the X-ray beam [21].

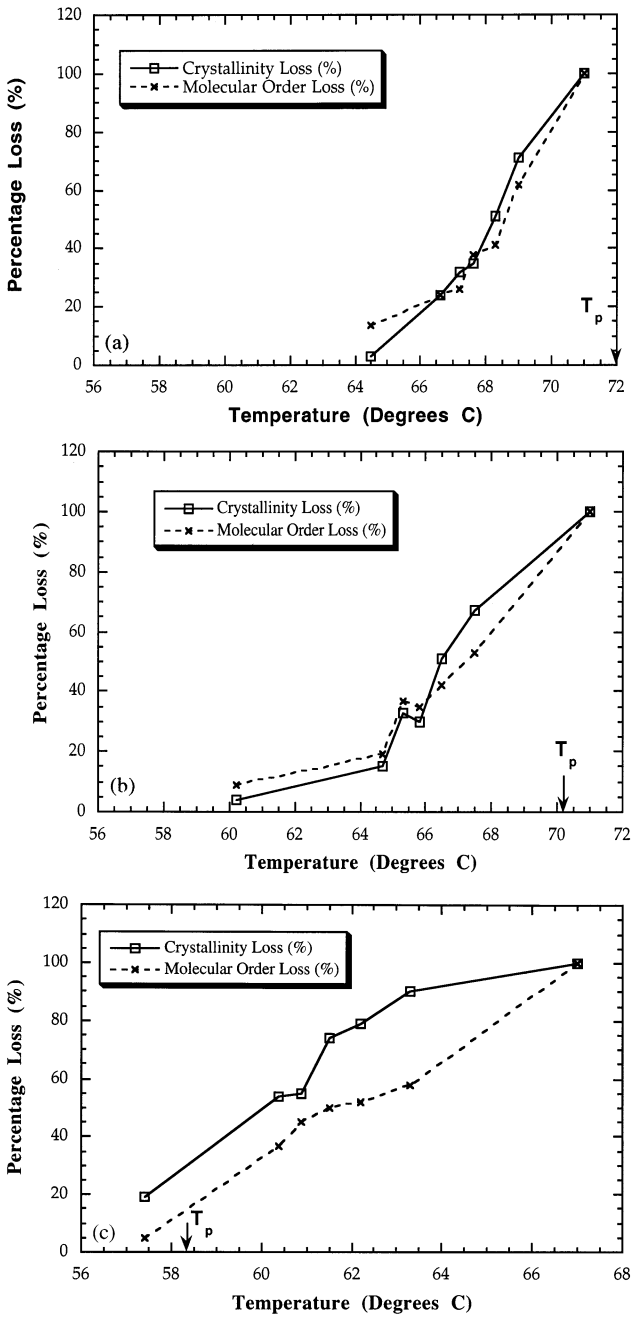

Fig. 1. (a) Comparison of crystallinity and molecular order loss from a series of retrograded waxy maize starches. T_p the peak endotherm temperature is shown. (b) Comparison of crystallinity and molecular order loss from a series of retrograded maize starches. T_p the peak endotherm temperature is shown. (c) Comparison of crystallinity and molecular order loss from a series of retrograded potato starches. T_p the peak endotherm temperature is shown.

'Molecular order' is a measure of helical content in the samples and was calculated as described by Gidley and Bociek [22] by decomposition of the spectra in terms of helical and amorphous references. Crystallinity loss is derived from measurements with a lab-based rotating anode X-ray source and is calculated using the Wakelin method [23].

3. Results

^{13}C CP/MAS solid state NMR data [16] is represented in Fig. 1(a–c) for retrograded starches gelatinised in excess water (20% w/w starch–water). Dynamic SAXS curves for potato, waxy maize, and maize are shown in Fig. 2(a–c). With B-type starches the variation of the 100 inter-helix reflection can be seen at 0.41 $Å^{-1}$ (Fig. 2(a)). SAXS from samples which had previously been slowly heated to the target temperature in excess water (5% w/w), cooled and then lyophilised are displayed in Fig. 3(a–d). Since maintaining a constant mass of starch (~ 50 mg) was difficult in all samples, an additional normalisation was carried out by requiring the high q regions to be equal. This is a regularly used method with SAXS normalisation; it does not change the behaviour if applied to the conventionally normalised samples of Fig. 2(a–c). A well defined 90 Å SAXS peak is shown by potato for intial heating temperatures $\leq$ 57.4 °C, waxy maize $\leq$ 68.3 °C, and maize $\leq$ 60.2 °C. An additional expanded picture of the 0.35–47 $Å^{-1}$ region of the SAXS curve for waxy maize (Fig. 3(c)) is shown in Fig. 3(b). It displays the appearance of the B-type polymorph after the SAXS peak has been completely lost at 71 °C in waxy maize starch. This appears to be a long time scale relaxation process not seen with samples examined directly after heat treatment [16].

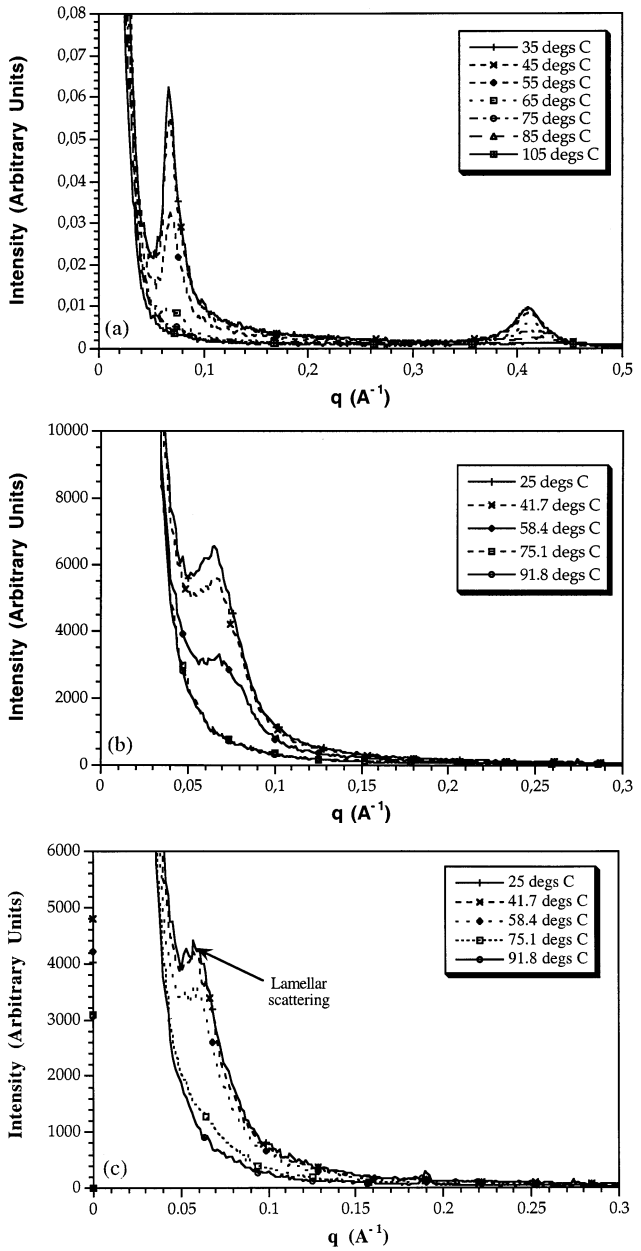

Fig. 2. (a) Curves taken during dynamic gelatinisation of potato starch (40% w/w) at the temperatures shown. Temperature ramp rate of 2 °C/min was used. (b) Dynamic gelatinisation of waxy maize starch (40% w/w). Temperature ramp rate of 2 °C/min was used. (c) Dynamic gelatinisation of maize starch (40% w/w). Temperature ramp rate of 2 °C/min was used.

The WAXS data that was collected is shown in Fig. 4(a–c). The WAXS data for maize starch is in good agreement with that published by Gidley et al for identical samples using a rotating anode source [16], although the other starches show signs of long term retrogradation due to their prolonged storage. Profiles were normalised by ensuring their integrated intensities were equal, that is the assumption of conserved scattered radiation [24]. A sharp change in the WAXS from A to B-type is seen for waxy maize at the point of gelatinisation 68.3–69.0 °C (Fig. 4(b)). This is just before the DSC peak endotherm of 72.2 °C detailed in Fig. 1(a). A more gradual change is seen with maize, and it occurs at a slightly lower temperature 65.3–67.3 °C. Considerable crystallinity loss is not observed in the normalised WAXS with potato starch in the range 57.4–67.0 °C. In common with the appearance of the B-type 100 peak in SAXS for waxy maize (Fig. 3(b)) the WAXS (Fig. 4(b)) indicated that a transformation from A-type to B-type unit cells occurs following initial heating up to 71 °C. An intermediate frustrated A-type structure of lower crystallinity occurs at the transformation point of 69 °C. It appears that some irreversible change can be associated with heating up to this temperature.

^{13}C CP-MAS NMR shows that in the maize samples shown in Fig. 1(a,b) there is a very sharp loss of both crystalline order, and molecular order during the final stage of gelatinisation. With potato starch the final rate of loss of crystalline order is much less (Fig. 1(c)), but the final loss of molecular order is greater than the crystallinity loss. The final stage of crystallinity loss is much smaller with potato (longer helices) 2.7%/°C, than with maize and waxy maize (shorter helices) 13.3, and 14.5%/°C, respectively. The final stages of molecular order loss are more similar with all three varieties: 11.4%/°C (potato), 19%/°C (waxy maize), and 13.4%/°C (maize).

If the waxy maize is only taken up to temperatures below 69 °C, recooling to rt allows the 90 Å peak to persist. This means that all the curves in Fig. 3(c) for the SAXS signal at rt after an initial heating to temperatures below 69 °C, superimpose on the uncooked data. The in-situ gelatinisation runs (Fig. 2(b)) show clearly that significant intensity has been lost in the 90 Å peak by the time the temperature has reached 58.4 °C. We postulate that Fig. 5 is the relevant model to describe this behaviour. At the lower temperatures there is a partial loss of crystallinity as double helices are stripped off the sides of the crystallites,

but they remain intact as double helices and if the temperature is dropped again the remaining crystal acts as a template on which the helices will partially relocate. However in the final stage of gelatinisation above 69 °C the molecular order losses (h) are large (note that Fig. 1(a) shows a change in gradient for the loss of both the helix content and crystallinity above this temperature) and it is suggested that above this temperature a helix–coil transition occurs. This corresponds to the temperature at which the WAXS signal is suddenly lost in Fig. 4(b). The persistence of the native 90 Å spacing upon subsequent cooling no

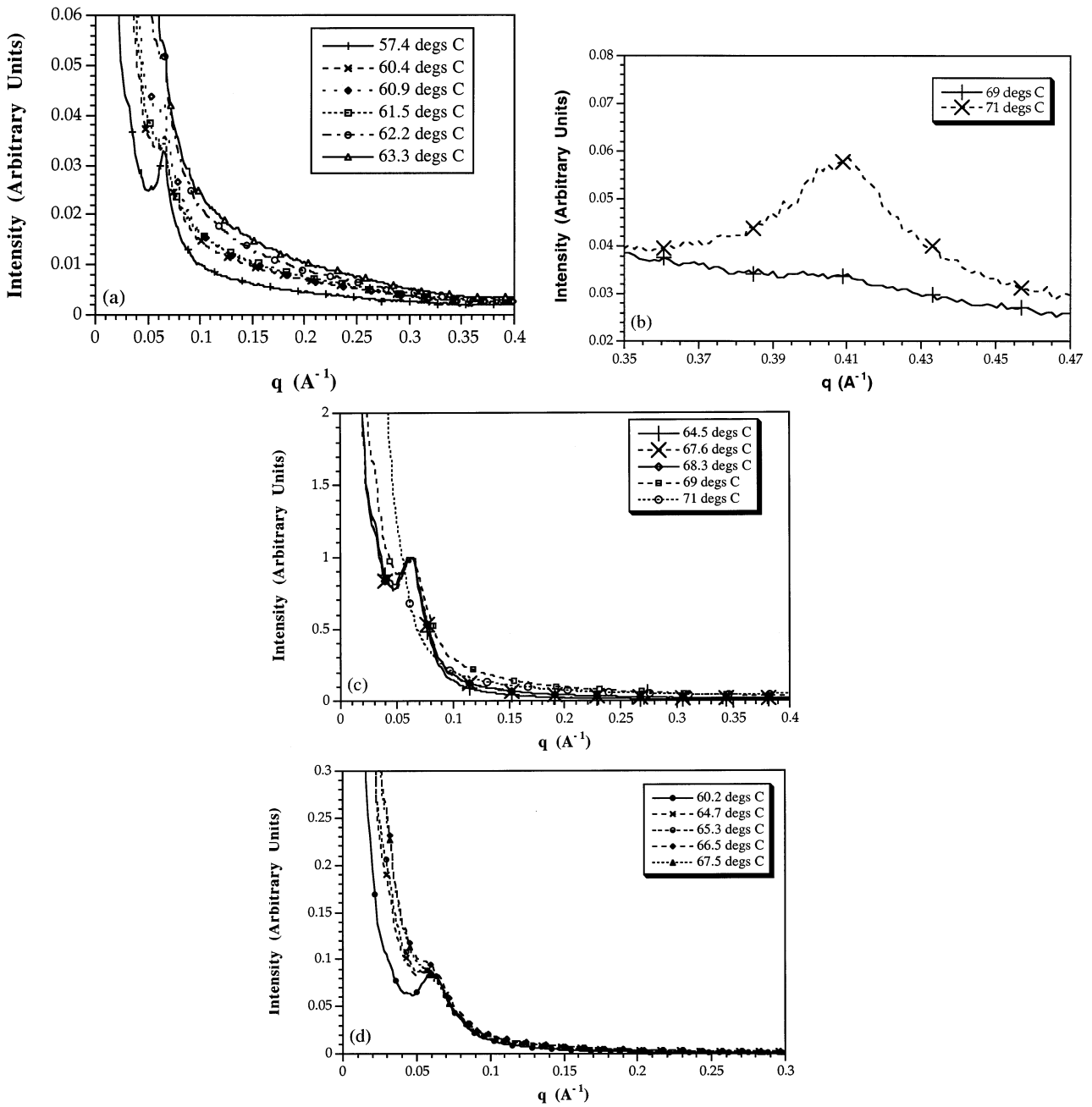

Fig. 3. (a) SAXS from retrograded potato starch. Samples were slowly heated to the target temperatures in excess water, and then cooled to room temperature. (b) Appearance of the 100 B-type reflection in retrograded waxy maize starch after long time storage at room temperature (>3 months). (c) SAXS from retrograded waxy maize starch. Samples were slowly heated to the target temperatures in excess water, and then cooled to room temperature. All the curves fall onto a single master curve below 69 °C. The relative normalisation is probably not quantitatively correct, since Fig. 1(c) shows a loss of helical content. (d) SAXS from retrograded maize starch. Samples were slowly heated to the target temperatures in excess water, and the cooled to room temperature.

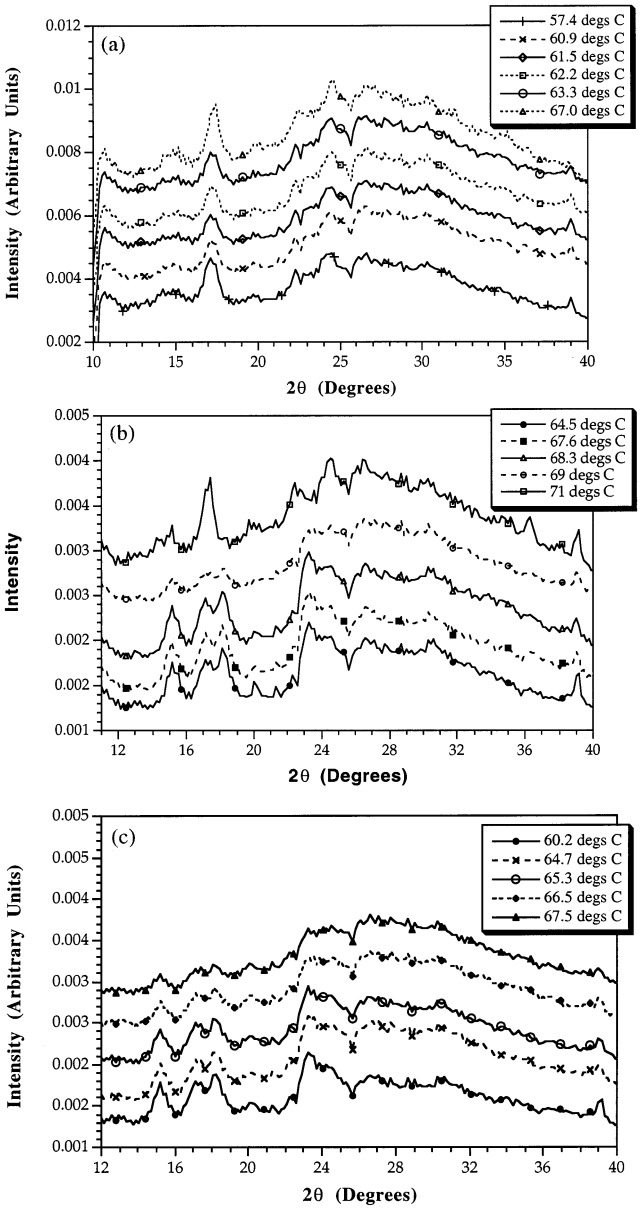

Fig. 4. (a) WAXS from retrograded potato starches. An additional offset has been applied to improve visibility. The data agrees with that found in Cooke and Gidley [16] except that the transition from B to A unit cells appears to be a long time scale transformation. (b) WAXS from retrograded waxy maize starches. An additional offset has been applied to improve visibility. Note that the unit cell changes at 71 °C from A to B type. The data agrees with Cooke and Gidley [16] except the A to B type transition assumes a long time scale behaviour. (c) WAXS from retrograded maize starches. An additional offset has been applied to improve visibility.

longer seems able to occur after this point, implying that whereas changes are reversible below this temperature, above it irreversible changes have occurred.

With the inclusion of amylose in waxy maize, that is 'normal type' maize, the temperature to which a sample can be heated, yet still maintain its SAXS periodicity on subsequent cooling and storage, is reduced (Fig. 3(d)). That is the thermal stability of the amylopectin lamellar structure is reduced by the linear polymer. The temperature at which maize maintains its SAXS periodicity drops to 60.2, 8 °C lower than the case with waxy maize, even though they have a similar amylopectin structure. We propose that amylose destabilises the lamellar crystallites causing their loss at lower temperatures by movement of the amylose molecules into regions containing amylopectin, thereby preventing the reformation of the original correlated structure.

Long term retrogradation in terms of recrystallisation into the B-type crystalline polymorph only occurs in amylopectin after the helix–coil transition with waxy maize. Below the temperature of this transition such a rearrangement cannot occur. Thus in Fig. 3(b) the (100) reflection only appears after the loss of the small angle peak at 69 °C. A similar transformation of A-type to B-type unit cells can be observed in the WAXS patterns of Fig. 4(b), but does not occur with the maize starches.

Solid state ^{13}C CP/MAS NMR evidence for the helix–coil transition is seen with all three samples in Fig. 1(a–c). The NMR data emphasises the helical nature of the sample (molecular order), since the technique only probes short-range interactions (< 10 Å) [25]. The loss of molecular helical ordering occurs at a similar rate for maize and waxy maize and more sharply than the loss of crystallinity during the final stages of gelatinisation for potato starch.

A piece of evidence supporting the idea of the importance of the helix–coil transition is seen in the relationship between the temperatures at which the crystallinity, the 100 B-type reflection and the SAXS peaks are lost in dynamic X-ray experiments. It has been universally found over a wide range of storage organ starches that the SAXS peak is lost before the final drop of the crystallinity index to zero [18]. The effect is seen in Fig. 6 with data derived from the dynamic gelatinisation of potato starch. Here as in previous studies, the SAXS peak and the 100 peak are lost at a

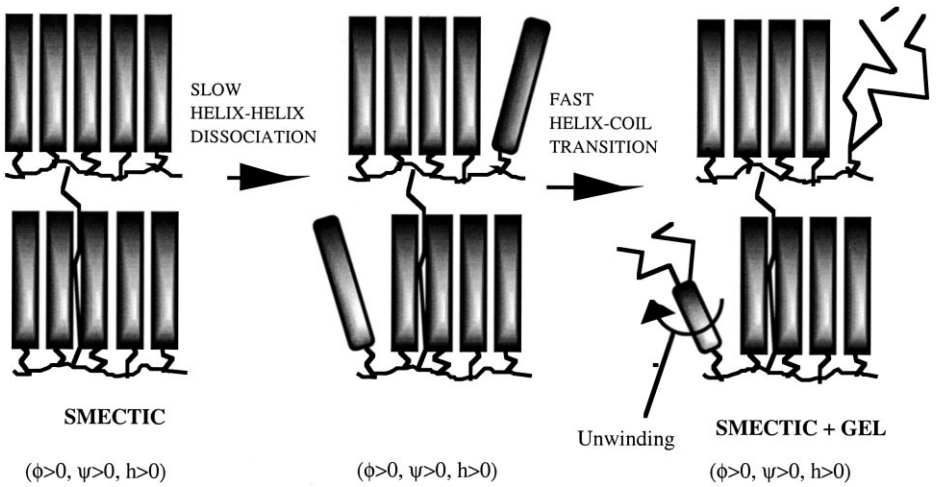

Fig. 5. The two-stage process involved in the gelatinisation of starch in excess water ($T_{hc} < T_{ss}$). The first stage involves a slow dissociation of the helices side-by-side. Immediately a helix coil transition occurs as a secondary effect. Relative values of the orientational (ϕ), lamellar (ψ), and helical order parameter (h) are included.

stage before the WAXS crystallinity index. This residual crystallinity is interpreted to be due to unmelted helices. Crystallinity indices deduced with the Wakelin method in starch [23] are thus a subtle combination of two types of phase transition, helix–helix dissociation and helix–coil transition (Fig. 5), whereas the SAXS and 100 peak measure the crystalline smectic–nematic transition alone (helix–helix dissociation). WAXS samples periodicities on the length scale of the wavelength used (1.54 Å), so even double helices which are not associated into crystallites can be expected to contribute to the scattering.

The shape of the curves in Fig. 1(c) for potato, are rather different from those for the A type starches of Fig. 1(a,b). Most of the order is lost beyond the peak in the gelatinisation endotherm rather than before, and the crystallinity loss occurs more rapidly than the loss of helical content. An explanation of the latter observation may be found from the consideration of the branch lengths of the amylopectin in the different species. In general the branch lengths in B-type starches such as potato are greater then for A-type, such as maize and waxy maize [4]. Consequently we may expect the length of double helices in potato also to be greater, and this will confer greater stability on them and hence make them resistant to dissociation. In this way it would be possible for three dimensional crystallinity to be lost, but not the order associated with the double helix structure. This would imply the existence of an intermediate nematic phase.

The 100 peak is also seen to broaden during dynamic gelatinisation of potato starch (Fig. 2(a)). A Gaussian can be fitted to the 100 peak isolated from the asymmetric background by subtraction of the fully gelatinised (amorphous) sample. The standard deviations of these Gaussian fits for potato starch are plotted against temperature in Fig. 7. They are larger at higher temperatures (vertical error bars). There are three factors that contribute to line broadening: microstrains, paracrystalline distortion and crystal size [24]. Assuming negligible thermal effects the

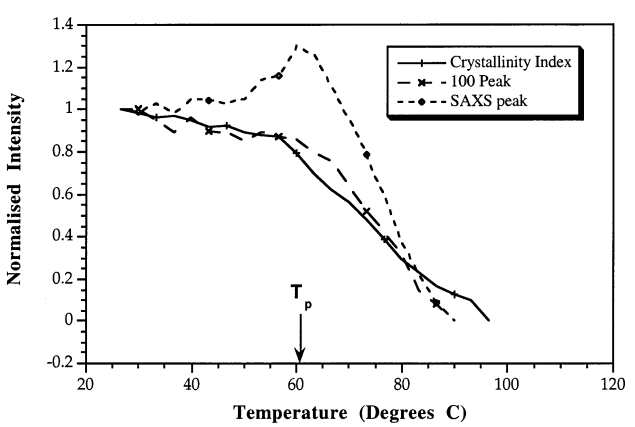

Fig. 6. Dynamic gelatinisation of potato starch (40% w/w). Showing the relative transition rates of the 100 peak, the SAXS peak, and the crystallinity index. The DSC peak endotherm temperature (T_p) is shown.

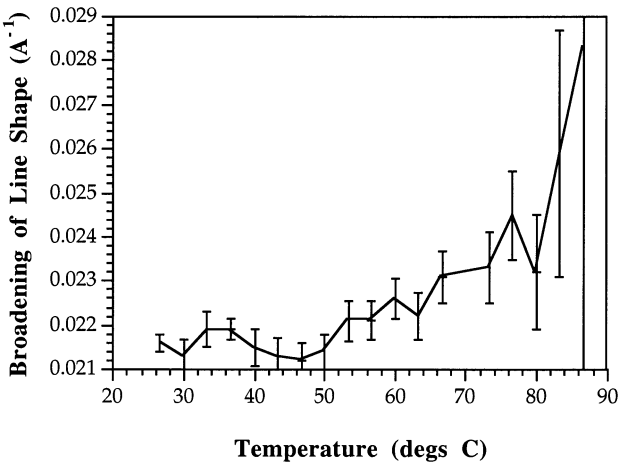

Fig. 7. The change in broadening of the 100 WAXS peak for potato starch during gelatinisation. Broadening of the profile corresponds to the standard deviation of a Gaussian fit. T_p is the peak endotherm temperature.

Debye–Waller factor (microstrains) will not change much in this temperature range (typically the thermal expansion coefficient is of the order of 2×10^{-4} K^{-1}, which gives a negligible contribution [24]), and it can be concluded that the double helices are pulling out of the crystallites producing either smaller crystallites (a Debye–Scherrer crystallite size term) or equally more distorted lamellae (paracrystalline broadening). This is again in agreement with a large scale transformation of all the crystallites during gelatinisation as the mosacity of the smectic crystallites increases and helices are lost.

4. Discussion

It is proposed that upon separation of the amylopectin double helices from their lamellar crystallites, a true helix–coil transition occurs. In their crystalline smectic packing [3,4], the amylopectin side chains intertwined in the double-helices strongly interact with not only their helical duplex partners, but with neighbouring chains in other helices. The dissociation of the double helices side by side is thus necessary to allow the unwinding transition, since it is otherwise geometrically impossible in the strongly interacting lamellar environment. Thus we invoke our first order parameter of the transitions involved during gelatinisation, the helicity of the sample. This is defined as the proportion of the paired monomers in the lamellae in the double helical state i.e., $h = N_h/(N_h + N_c)$, N_h is the number in the helical state and N_c is the number in the coil state. The molecular order losses measured using ^{13}C NMR in Fig. 1(a–c) could be considered a first approximation to this value of h.

Drawing together ideas in the literature there are four scenarios for the denaturation of helices which need to be considered: crystalline, concentrated (e.g., nematic, smectic, isotropic), semi-dilute, and dilute. Dilute helices, with non-interacting solution state components, are commonly the subject of Zimm–Bragg theories [19,20]. In semi-dilute solutions there is thought to be both entropic and enthalpic stabilisation of the double helices. Short regions of helix are stabilised at much higher temperatures if they interact side-by-side [26,27]. Zimm–Bragg theories including corrections for loops and inter-helix interactions, predict an initial dissociation of helices side by side followed by immediate dissociation of helices during the final collapse of these semi-dilute helices. In the concentrated regime, stabilisation of alpha helices is possible due to the excluded volume of their neighbours. This phenomena is encapsulated in the 'induced rigidity effect' [28], where helices are stabilised to higher temperatures in the nematic state (entropic stabilisation) i.e., fluctuations in the helices are inhibited by the geometrical constraints of their neighbours. In the crystalline state direct melting of the helices into the coil state can occur as observed with amylose crystallites (enthalpic stabilisation) [29]. Thus we see the importance of considering the helical order parameter in relation to two other order parameters [30]. Firstly there is the orientational order of the helices which characterises the nematic phase behaviour e.g., $\phi = 1/2(3\cos^2\theta - 1)_V$ and can be measured by birefringence or microfocus X-ray scattering [2], where θ is the angle between the mesogen's director and the average orientational alignment of the mesogen ensemble. Secondly there is the lamellar order parameter which measures the tendency to form periodic structures in one dimension. For example we have $\rho = \rho_0(1 + \psi\cos(2\pi z/d))$,

the amplitude of the first Fourier component of a periodic density modulation, z is the lamellar perpendicular, d is the lamellar period, ρ_0 is the average electron density and ρ is the electron density. Here ψ, the order parameter, is measurable by SAXS and a rough approximation would be the peak heights calculated in Fig. 6.

The analysis for the case of amylopectin is slightly different to a normal Zimm–Bragg theory of double helix coil transition, since two of the ends of the polymers constituting the helical duplex are connected together. In such models this will only change the value of the free energy for helix nucleation (make it more likely) and not affect the cooperativity or broadening of the transition as a function of the length of the helix (n). It is predicted for models of short chain double helical hairpins that the dissociation occurs from the ends, and not the hair pin at the branch point [20] (Fig. 8). Past the point of dissociation it is hypothesised that the free ends of the amylopectin helices mix up producing topological constraints, discouraging the re-assembly of the double helices. They can now re-associate with parts of amylopectin molecules other than their original helix duplex partner, forming physical junctions (new double helices)

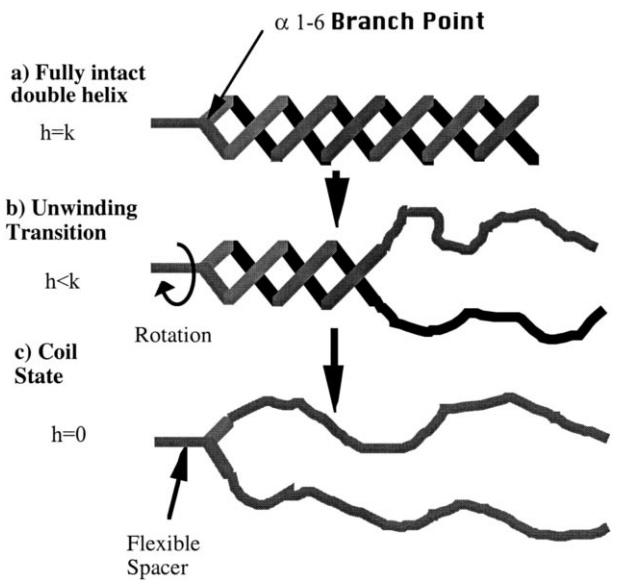

Fig. 8. The helix–coil transition in amylopectin double helices. Unwinding occurs from the loose ends, and not at the hairpin due to entropic effects. Relative values of the helical order parameter (h) are included, k is its value when the helix is completely associated.

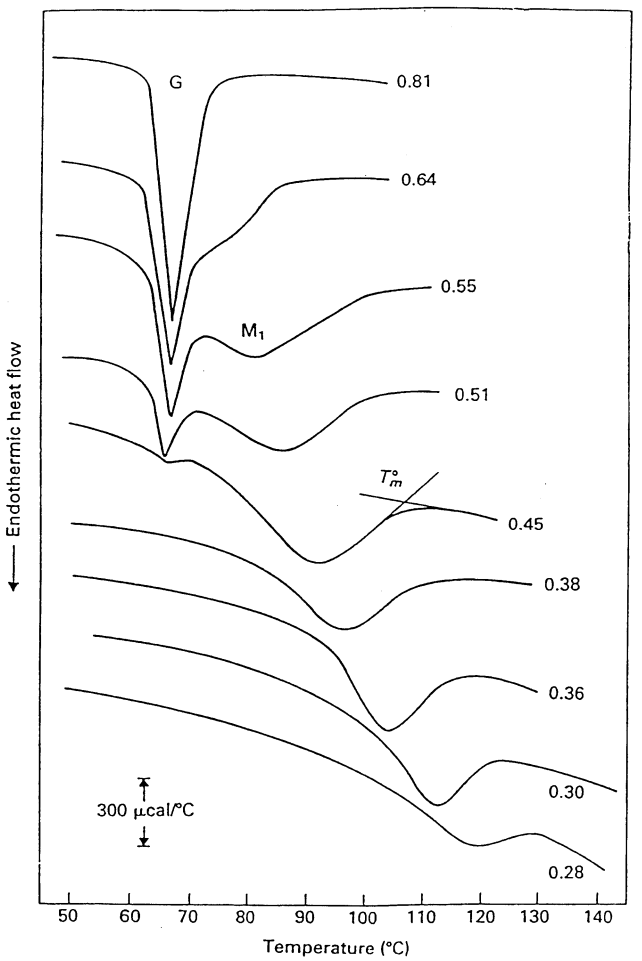

Fig. 9. Differential scanning calorimetry profiles of potato starch at various solvent fractions (a volume of 0.6 corresponds to about 50%). The heating rate was 10 °C/min. Adapted from Donovan [11].

and creating more general amorphous hydrogen bonded associations. Possible rotation of the helices as they unwind will be a kinetic limiting step for the unwinding transition. The ease of rotation of the links of the flexible spacer attached to the amylopectin double helix could thus affect the rate of gelatinisation, i.e., long spacers (A-type) encourage rapid dissociation due to their increased flexibility [31].

This model of helix–helix dissociation followed by a helix–coil transition provides a framework within which to understand the water content dependent DSC traces of starch gelatinisation, e.g., Fig. 9 for potato starch. In excess water ($>40\%$ w/w) the difference between the DSC endotherms of the crystalline smectic/nematic (smectic–isotropic with A-type), and helix–coil transition are presumed

to be immeasurably small (Fig. 5). In other words the ultimate loss of the smectic crystals is assumed to occur simultaneously with helix dissociation. However it is well known that upon decreasing the water content to 40% w/w two endotherms are observed. We postulate that the first endothermic event is due to the crystalline smectic–nematic phase transition, and the second is the unwinding transition of the helices (Fig. 10(i)). Decreasing the amount of water still further a direct glassy nematic to gel transition occurs as the helices unwind. Inter-crystalline B to A phase transitions can also occur at low water contents which is a further complicating factor [32].

The first DSC endotherm has been observed to be sensitive to sample annealing in SAXS, WAXS, and DSC experiments [33]. It is probably connected to the rearrangement of the dislocations in the tilted lamellar structures [3], permitting an improvement in overall order. However the invariance of the second endotherm to annealing behaviour is what is expected for a helix–coil transition, since the nature of the consistent helices (their length, cohesive energy, etc.) is not changed by heating below their unwinding transition.

Elevation of the helix–coil transition temperature as the water content is reduced could be explained by invoking a larger value of ΔF_s (free energy change for the junction between a

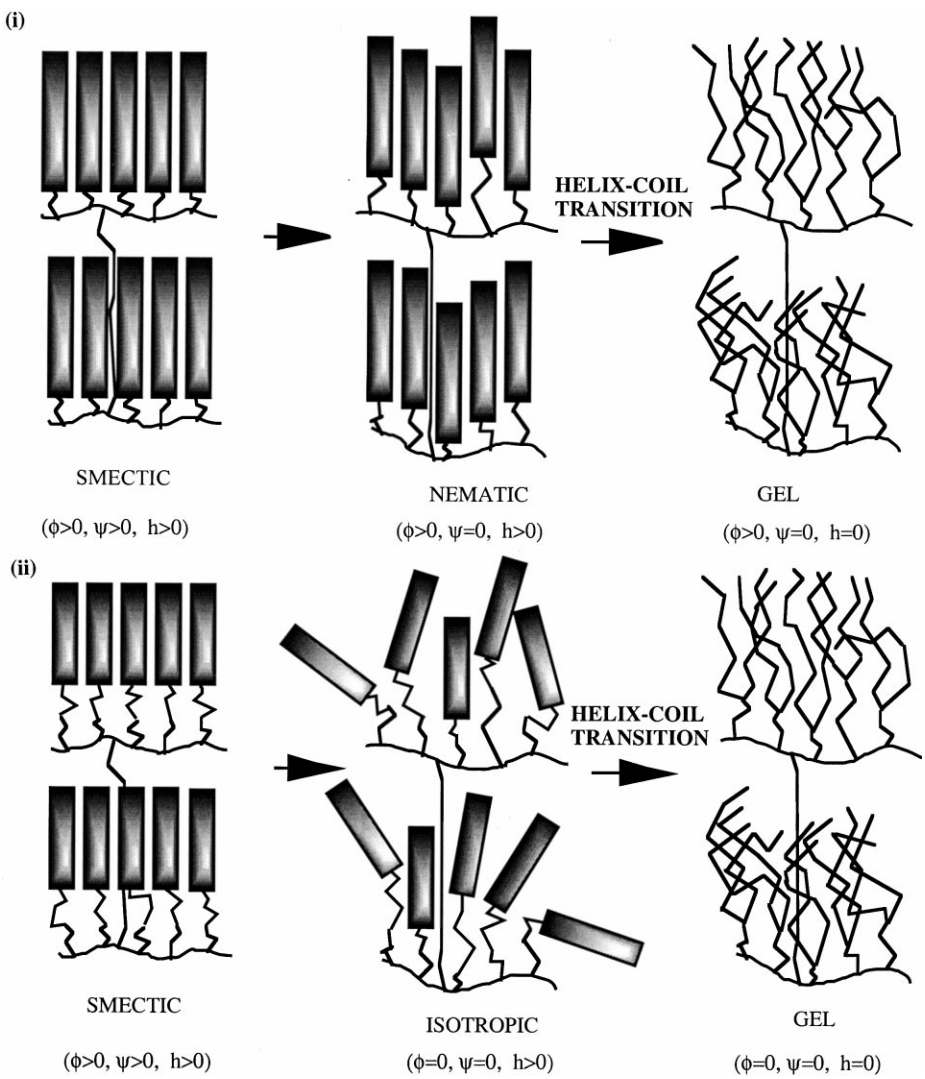

Fig. 10. The two-stage process involved in the gelatinisation of starch in limiting water. Two different processes are shown for A and B type starches. It is proposed that the intermediate phase is determined by the length of the amylopectin helices. Relative values of the orientational (ϕ), lamellar (ψ), and helical order parameter (h) are included. (i) In B-type starch the intermediate phase is nematic in character, (ii) and in A-type starch the intermediate phase is isotropic in character.

helix and coil state) in a Zimm–Bragg model [19]. That is the helix state becomes more favourable compared to the coil state at higher temperatures. The second endotherm in limiting water which is presumed to be associated with the helix–coil transition, is broader in A-type (wheat) starches than with B-type (potato) in agreement with Zimm–Bragg models as regards to the length of the helix: this is greater with B-type [19].

In limiting water it is postulated that the temperature at which the unassociated helix–coil transition of the amylopectin double helices would take place (T_{hc}) is greater than the temperature for the dissociation of helices side-by-side in their crystallites (T_{ss}) i.e., $T_{hc} > T_{ss}$. The balance between these two processes is determined by the amount of available water for plasticisation of the amorphous backbone, and spacers, and for the dissociation of the double helices in to the coil state. In a later paper we will discuss in more detail the importance of plasticisation for organisation of the smectic layers, and hence for the perfection of packing.

A two stage process for the changes experienced by the lamellae in limiting water can then be proposed. As the system is heated the thermal energy eventually becomes sufficient to break the inter-mesogen hydrogen (10–40 kJ mol^{-1}) bonds [34] to increase the mobility of the amylopectin double helices side-by-side. Thus the SAXS peak is lost through a smectic ($\phi > 0$, $\psi > 0$, $h > 0$) to nematic/isotropic phase change ($\phi > 0/ = 0$, $\psi = 0$, $h > 0$ Fig. 10 (i,ii)). Adding yet further heat, the helices unwind through their extremely cooperative transition and birefringence of the granule is lost ($\phi = 0$, $\psi = 0$, $h = 0$). There are two DSC endotherms [11], because the lamellar order parameter (ψ) is lost in the crystalline smectic to isotropic/nematic transition at lower temperatures, and then the helix–coil transition (h) occurs at higher temperatures. Zimm–Bragg models predict that the broadening of the thermodynamic transition is inversely proportional to the double helix length [35]. This is in qualitative agreement with DSC data in which the second endotherm for A-type starches (shorter helices) is seen to be broader than that of B-type (longer helices) [11]. The intermediate phase for A-type starch is designated isotropic, since it is not birefringent. The longer amylopectin helices in B-type starches stabilise an intermediate nematic phase due to their increased aspect ratio compared to A-type starches where the intermediate phase is isotropic.

It should be noted that lamellar swelling is only possible once the smectic to nematic/isotropic transition has occurred. Otherwise the lamellar periodicity would need to change which is not observed in Figs. 2 and 3. This provides an explicit molecular mechanism for the 'swelling driven processes' alluded to by previous authors in the field [1,14,16].

In excess water the temperature at which an unassociated helix to coil transition would take place (T_{hc}) and the temperature for dissociation of helices side-by-side in their crystallites (T_{ss}) are either similar or the helix-to-coil transition is lower i.e., $T_{hc} \leq T_{ss}$. There are thus two subtly different scenarios I and II:

1. $T_{hc} < T_{ss}$. The amylopectin double helices can only unwind if they are dissociated from their crystallites (Fig. 5). Therefore even if T_{hc} is lower than T_{ss} before the transition temperature the double helices will be prohibited from realising their own localised free energy minima. Hence as the temperature is increased an endotherm occurs only as the helices dissociate side-by-side (slow), and the helix coil transition happens as an immediate consequence of this step (fast). The endotherms therefore merge together.
2. $T_{hc} \approx T_{ss}$. Here it is postulated that a similar process occurs as with limiting water (Fig. 10). There is a smectic–nematic/isotropic transition followed by the helix unwinding transition.

In reality both of the two processes I and II could be in effect. Although with A type starches we can deduce that I) is the predominant process, because the DSC peak endotherm occurs at the point of complete loss of helical ordering (Fig. 1(a,b)). With B-type starches the DSC endotherm (Fig. 1(c)) occurs well before the final loss of helices showing an increased contribution of process II). The De Gennes–Pincus [28] induced rigidity effect

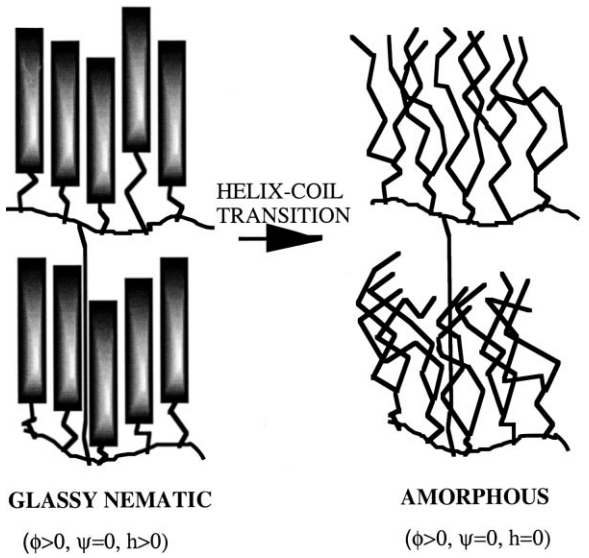

Fig. 11. The single stage process involved in the gelatinisation of starch at low water contents. The transition shown is for B-type starch and it transforms from the glassy nematic to the amorphous state. Relative values of the orientational (ϕ), lamellar (ψ), and helical order parameter (h) are included.

may well be contributing to helical stability in the B-type case, during a broad intermediate nematic phase.

With B-type/A-type starch the sample is initially in the glassy nematic/crystalline state, respectively, at room temperature. A direct helix to coil phase change occurs with both sample types at elevated temperatures (Fig. 11). The mobility of the backbone and spacers is not sufficient to stabilise a mobile nematic phase, and only a single endotherm occurs in the DSC trace [11].

Acknowledgements

T.W. would like to thank the BBSRC and Unilever Research for a CASE award to fund his PhD.

References

[1] J.M.V. Blanshard, in T. Galliard (Ed.), *Starch Properties and Potential*, Wiley, New York, 1987.
[2] T.A. Waigh, I. Hopkinson, A.M. Donald, M.F. Butler, F. Heidelbach, C. Riekel, *Macromolecules*, 30 (1997) 3813–3820.
[3] T.A. Waigh, A.M. Donald, F. Heidelbach, C. Riekel, M.J. Gidley, *Biopolymers*, 49 (1999) 91–105.
[4] T.A. Waigh, P.A. Perry, C. Riekel, M.J. Gidley, A.M. Donald, *Macromolecules*, 31 (1998) 7980–7984.
[5] D. French, in R.L. Whistler, J.N. BeMiller, E.F. Paschall (Eds.), *Starch: Chemistry and Technology*, Vol. 2, Academic Press, London, 1984, pp. 183–247.
[6] A. Imberty, S. Perez, *Int. J. Biol. Macromol.*, 11 (1988) 177–185.
[7] A. Imberty, A. Buleon, V. Tran, S. Perez, *Starch*, 43 (1991) 375–384.
[8] P.J. Jenkins, R.E. Cameron, A.M. Donald, *Starch*, 45 (1993) 417–420.
[9] T. Galliard, in T. Galliard (Ed.), *Starch: Properties and Potential*, Wiley, New York, 1987.
[10] M. Yamaguchi, K. Kainuma, D.J. French, *J. Ultra. Res.*, 69 (1979) 249–261.
[11] D.W. Donovan, K. Lorenz, K. Kulp, *Cereal Chem.*, 60 (1983) 381–387.
[12] P.J. Jenkins, R.E. Cameron, A.M. Donald, V.M. Bras, G.E. Derbyshire, G.R. Mant, A.J. Ryan, *J. Polym. Sci. B: Polym. Phys.*, 32 (1994) 1579–1583.
[13] T.A. Waigh, P.J. Jenkins, A.M. Donald, *Faraday Discuss.*, 103 (1996) 325–337.
[14] M.T. Kalichevsky, E.M. Jaroszkiewicz, S. Ablett, J.M.V. Blanshard, P.J. Lillford, *Carbohydr. Polym.*, 18 (1992) 77–88.
[15] J. Lelievre, *J. Appl. Polym. Sci.*, 18 (1973) 293–296.
[16] D. Cooke, M.J. Gidley, *Carbohydr. Res.*, 227 (1992) 103–112.
[17] T. Shiotsuab, K. Takahashi, *Agri. Biol. Chem.*, 48 (1984) 9.
[18] P.J. Jenkins, A.M. Donald, *Carbohydr. Res.*, 208 (1998) 133–147.
[19] B.H. Zimm, J.K. Bragg, *J. Chem. Phys.*, 31 (1959) 526.
[20] D. Poland, H.A. Scheraga, *Theory of Helix–Coil Transitions in Biopolymers*, Academic Press, New York, 1970.
[21] W. Bras, G.E. Derbyshire, A.J. Ryan, G.R. Mant, P.K. Murry, K. Roberts, I. Sumner, J.S. Warges, R.A. Lewis, A. Gabriel, *Rev. Sci. Instr.*, 60 (1989) 2346.
[22] M.J. Gidley, S.M. Bociek, *J. Am. Chem. Soc.*, 107 (1985) 7040–7044.
[23] J.H. Wakelin, H.S. Virgin, E. Crystal, *J. Appl. Phys.*, 30 (1959) 1654–1662.
[24] F.J. Balta-Calleja, C.G. Vonk, *X-ray Scattering of Synthetic Polymers*, Elsevier, Amsterdam, 1989.
[25] V.J. Mcbrierty, K.J. Packer, *Nuclear Magnetic Resonance in Solid Polymers*, Cambridge University Press, Cambridge, 1993.
[26] J. Skolnick, A. Holtier, *Macromolecules*, 15 (1982) 3033.
[27] W.L. Mattice, *Biopolymers*, 24 (1985) 2231–2242.
[28] P.G. de Gennes, P. Pincus, *Polym. Prepr. Am. Chem. Soc.*, 18 (1977) 161.
[29] G.K. Moates, T.R. Noel, R. Parker, S.G. Ring, *Carbohydr. Res.*, 298 (1997) 327–333.
[30] P.M. Chaikin, T.C. Lubensky, *Principles of Condensed Matter Physics*, Cambridge University Press, Cambridge, 1995.
[31] A. Buleon, V. Tran, *Int. J. Biol. Macromol.*, 12 (1990) 345–352.
[32] P. Colonna, A. Buleon, C. Mercier, in T. Galliard (Ed.), *Starch: Properties and Potential*, Wiley, New York, 1987, pp. 79–114.
[33] H. Jacobs, N. Mischenko, M.H.J. Koch, R.C. Eerlingen, J.A. Delcour, H. Reynaers, *Carbohydr. Res.*, 306 (1998) 1–10.
[34] J. Israelachvili, *Intermolecular and Surface Forces*, Academic Press, New York, 1992.
[35] A.Y. Grosberg, A.R. Khokhlov, *Statistical Physics of Macromolecules*, AIP Press, New York, 1994.